

PAPER • OPEN ACCESS

CFD modeling and experimental verifications of a four-stage Stirling-type pulse tube cryocooler

To cite this article: Rui Zha *et al* 2019 *IOP Conf. Ser.: Mater. Sci. Eng.* **502** 012037

View the [article online](#) for updates and enhancements.

CFD modeling and experimental verifications of a four-stage Stirling-type pulse tube cryocooler

Rui Zha^{1,2,*}, Tao Zhang^{1,2}, Jiaqi Li^{1,2}, Jun Tan^{1,3}, Yongjiang Zhao^{1,2}, Bangjian Zhao^{1,2}, and Haizheng Dang^{1,3,**}

¹ State Key Laboratory of Infrared Physics, Shanghai Institute of Technical Physics, Chinese Academy of Sciences, 500 Yutian Road, Shanghai 200083, China

² University of Chinese Academy of Sciences, No. 19A Yuquan Road, Beijing 100049, China

³ Shanghai Boreas Cryogenics Co., Ltd, 1388 Shuidian Road, Shanghai 200434, China

*Corresponding author: cryoray@163.com

**Corresponding author: haizheng.dang@mail.sitp.ac.cn

Abstract. This paper conducts CFD modeling and experimental verifications of a four-stage Stirling-type pulse tube cryocooler (SPTC) aimed to reach liquid helium temperature for low T_c superconducting devices and deep space exploration. A two-dimensional (2-D) axis-symmetric CFD model with the thermal non-equilibrium mode is developed to simulate the internal operating mechanism. A cryogenic phase-shifting approach is employed to improve the phase conditions. Several cases are set to study the phase relationship between mass flow rate and dynamic pressure at the inlet and outlet of the regenerator. The effects of the operating frequency on flow and heat transfer processes in the pulse tube are also investigated. Based on the above numerical studies, a four-stage thermally-coupled SPTC is then developed and tested. It reaches a no-load temperature of 4.5 K and achieves cooling capacities of 10.5 W/ 80 K, 8.6 W/ 60 K, 1.5 W/ 30 K and 10 mW/ 5 K experimentally.

1. Introduction

The SPTC, driven by linear compressor based on flexure springs and clearance seal, achieves significant advantages such as high reliability, low vibration and long operation time, and thus plays an important role in many special fields including aerospace, military defense and superconducting, etc. At present, single-stage SPTCs have already been widely used in practical applications with cooling temperatures of above 25 K, and two-stage ones with cooling powers simultaneously at both stages, normally varying between 20 K and 180 K, are also becoming mature [1-2]. In recent years, three-stage SPTCs are developed to provide cooling at below 20 K for low- T_c superconducting devices and deep space explorations. Olson et al. [3] reported a three-stage SPTC and achieved a no-load temperature of 10 K. Wilson and Gedeon [4] developed a three-stage gas-coupled SPTC with a no-load temperature of 5.5 K. Dang et al. [5] conducted a thermally-coupled three-stage SPTC and investigated the effect of a cryogenic phase-shifter.



Table 1. Geometrical dimensions and boundary conditions of each component.

Component	Diameter (mm)	Length (mm)	Boundary condition
Reg I	14	38	Adiabatic
Reg II	12	28	Adiabatic
Reg III	12	26	Adiabatic
Reg IV	12	39	Adiabatic
PHX I	-	5	80 K
PHX II	12	5	40 K
PHX III	12	5	25 K
Pulse tube	8	80	Adiabatic

The four-stage SPTC is a promising cryocooler candidate for directly achieving the liquid helium temperature. It can also provide four different cooling temperatures varying from 120 K to 4 K for various applications simultaneously, which is more compact and economical compared to multiple cooling systems. So far, few researches on the four-stage SPTC are reported. Olson et al. [6] developed a four-stage SPTC to provide cooling at 6 K and 18 K, driven by a linear moving-magnet compressor. Nast et al. [7] built a split four-stage SPTC and reached a no-load temperature of 3 K.

Most previous studies focused on structure design, practical manufacture and performance optimization of the multi-stage SPTC, whereas the in-deep theoretical analyses of the inner process and operating mechanism are rarely conducted. The four-stage SPTC has much more complicated physical structure and operating mechanism than those of single-, two- or three-stage ones. The staging configurations of the four-stage SPTC result in the flexibility to change the various stage cooling temperatures and capacities for different applications.

This paper will develop a 2-D axis-symmetric CFD model of a four-stage SPTC. The effects of the cryogenic phase-shifter temperature and operating frequency will be investigated in depth. A four-stage thermally-coupled SPTC will then be developed to verify the theoretical studies. The simulated and experimental results will be compared and discussed in detail.

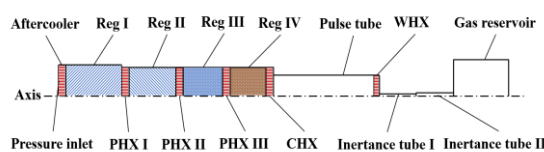
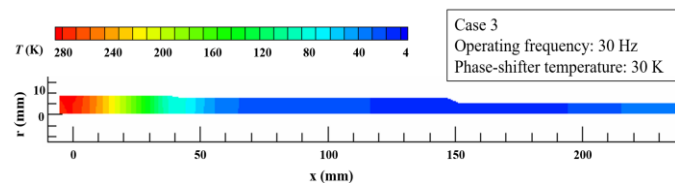
Table 2. Parameters setting in different cases

Case	1	2	3	4	5	6	7	8	9	10
Phase-shifter temperature (K)	20	25	30	35	40	30	30	30	30	30
Operating frequency (Hz)	30	30	30	30	30	26	28	30	32	34

2. CFD modeling

The 2-D axis-symmetric geometry of the fourth stage is shown in figure 1. The regenerator has four segmented parts packed with 400# stainless steel (SS) meshes, 635# SS meshes, Er₃Ni and HoCu₂, respectively. Table 1 gives the geometric dimensions and boundary conditions of these components.

A second-order upwind scheme is applied in this model to solve the continuity, momentum and energy equations. The various cases simulated in this model are listed in table 2. Case 1-5 are set to investigate the effect of the temperature of cryogenic phase-shifter with operating frequency at 30 Hz. Then case 3, case 6-10 are used for predicting the cooling performance when the operating frequency is varying from 26 Hz to 36 Hz.

**Figure 1.** 2-D axis-symmetric geometry of the fourth stage cold finger.**Figure 2.** Temperature contour in the CFD model for case 3.

3. Results and discussion

3.1 Cryogenic phase-shifter

The temperature contour in the model for case 3 is shown in figure 3. Figure 2 indicates the detailed temperature distribution for case 3 in axial direction. A no-load cycle-averaged temperature of 4.0 K is achieved with three precooling temperatures of 80 K, 40 K and 25 K.

Case 1-5 are employed to find the optimal temperature of the cryogenic phase-shifter. Figure 3 (a)-(c) shows temporal variations of the dynamic pressure and mass flow rate at the inlet and outlet of the regenerator for case 1, case 3 and case 5, which phase-shifters are at 20 K, 30 K and 40 K, respectively. The amplitude of the mass flow rate at the outlet of the regenerator increases with the growth of the phase-shifter temperature T_{ps} , whereas the one at the inlet hardly changes.

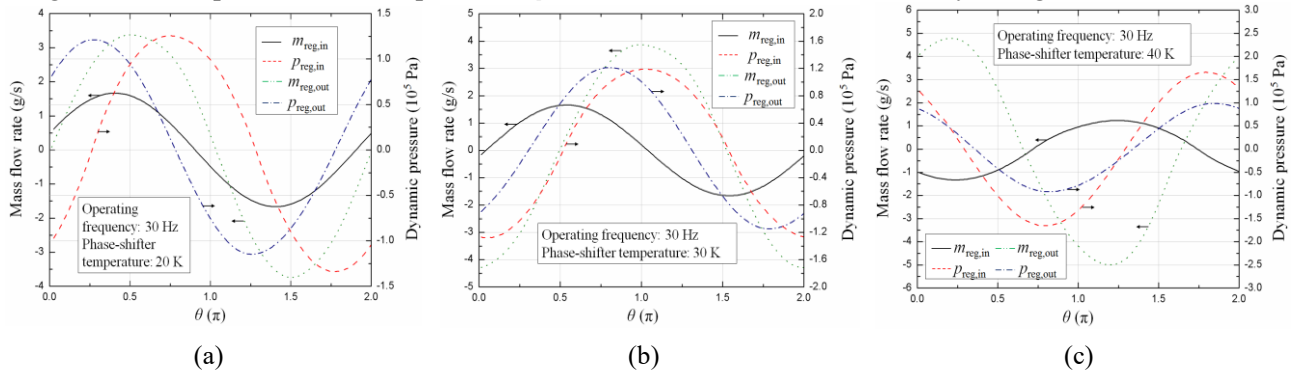


Figure 3. Dynamic pressure and mass flow rate at inlet and outlet of regenerator. (a) Case 1. (b) Case 3. (c) Case 5.

Figure 4 shows the no-load temperature and the phase angle at the inlet and outlet of the regenerator as a function of T_{ps} . According to the results, the phase-shifter temperature significantly affects the phase conditions. The optimal temperature is 30 K and a time-averaged no-load temperature of 3.8 K is achieved. Whether T_{ps} rises or falls results in worse performance. The phase angle is -35.0° at the outlet of the regenerator when $T_{ps}=30$ K, and then increases to -39.6° and -44.5° when $T_{ps}=20$ K and 40 K, respectively. At the inlet of the regenerator, the phase angle increases from 60.2° to 89.9° with the growth of T_{ps} and when $T_{ps}>30$ K, it increases more quickly. The phase relationship between mass flow rate and dynamic pressure changes with the variation of phase-shifter temperature and thus affects the cooling performance of the fourth stage.

Temperature contours inside the pulse tube in case 1-5 at the same moment are shown in figure 5. Obviously, two-dimensional flow occurs in the pulse tube when the phase-shifter is at different temperatures. In case 3, the flow remains static practically. In case 1 and case 5, the streaming is almost through the whole pulse tube. The isotherms are nearly horizontal in the middle of the pulse tube, which means the gas displacer is destroyed and fluids at two ends can't be isolated effectively.

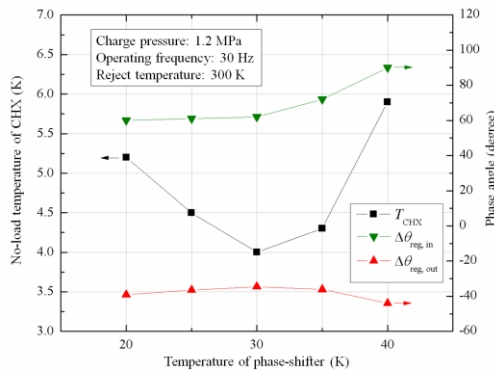


Figure 4. No-load temperature and phase angle.

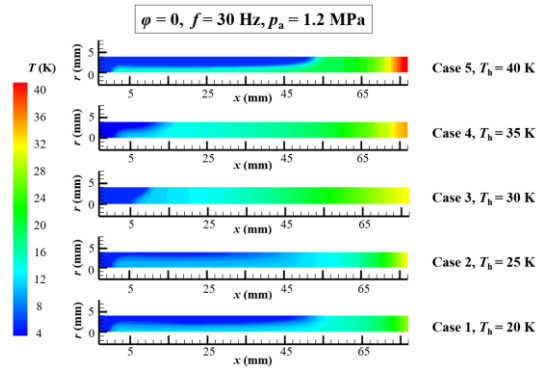


Figure 5. Temperature contours inside pulse tube.

3.2 Effect of operating frequency

The temperature contours inside the pulse tube during one cycle at different operating frequencies are shown in figure 6 (a)-(c). It is evident that either higher or lower operating frequency would lead to a worse performance than that at the optimal frequency. In case 6 at 26 Hz shown in figure 6 (a), the isotherms distort at both ends of the pulse tube, in which the right side is much more severe. During the process of expansion, the warm fluid near the axis flows into the CHX and make its temperature even higher than the fluid near the wall. In case 3 shown in figure 6 (b), the temperature distortion is more moderate than in case 6. When the frequency increases to 36 Hz, the flow condition becomes more complex. Obviously, several vortices are fully developed in the pulse tube and then deteriorate the cooling performance.

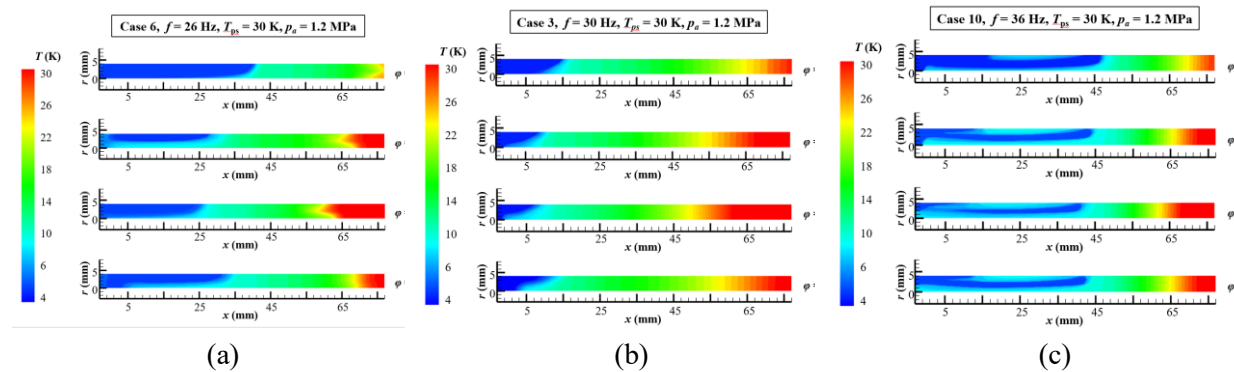


Figure 6. Temperature contour inside pulse tube during one cycle. (a) Case 6. (b) Case 3. (c) Case 10.

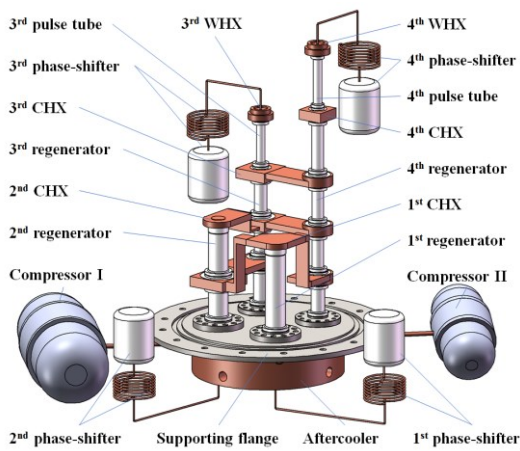


Figure 7. Configuration of four-stage SPTC.

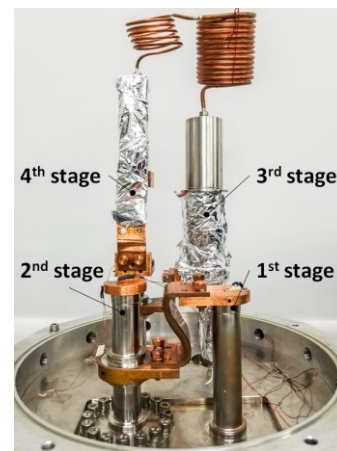


Figure 8. Structure of cold finger.

4. Experimental verifications

To verify the validity of the above results, a four-stage thermally-coupled SPTC is developed and tested. The configuration of the SPTC is shown in figure 7 and figure 8, and the experimental setup is displayed in figure 9. It is driven by two linear compressors developed in the same group. The first and second stages are driven by one compressor and the third and fourth stages by the other one. The best performance achieves at 30 Hz in both simulations and experiments, which verifies the veracity of the CFD model. Figure 10 shows the cool-down curves of the four stages. It takes about 160 minutes for the whole system to be steady. The final no-load temperatures of the four stages are 63.54 K, 42.18 K, 25.20 K and 4.50 K, respectively. More tests were carried out to evaluate its ability of simultaneous cooling at four different temperatures. According to the results, the four-stage SPTC can achieve cooling capacities of 10.5 W/ 80 K, 8.6 W/ 60 K, 1.5W/ 30 K and 10 mW/ 5 K.

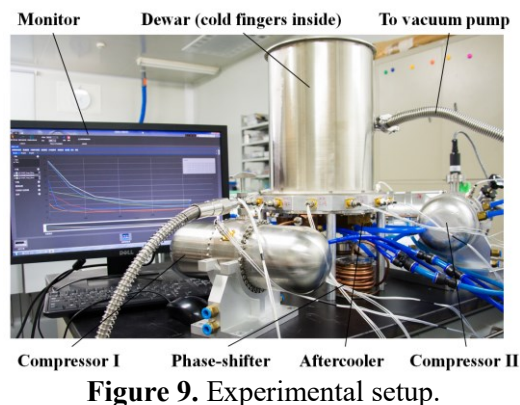


Figure 9. Experimental setup.

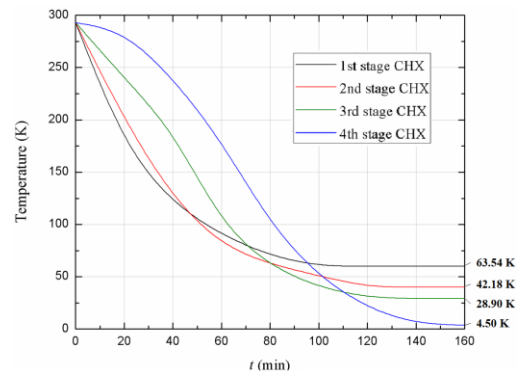


Figure 10. Cool-down curves of each stage.

5. Conclusions

This paper conducts CFD modeling and experimental verification of a four-stage SPTC aimed to provide efficient cooling capacities at four different temperatures. A 2-D axis-symmetric CFD model of the fourth stage is developed to investigate phase conditions and oscillating flows in the regenerator and the pulse tube.

The phase angles between mass flow rate and dynamic pressure at the inlet and outlet of the regenerator with phase-shifter temperatures of 20 K, 25 K, 30 K, 35 K and 40 K are investigated. The results indicate that the fourth stage achieves the best cooling performance when the phase-shifter temperature is 30 K. The effects of the operating frequency ranging from 26 Hz to 36 Hz on the performance are studied in detail. The optimal frequency is 30 Hz for the fourth stage.

A four-stage thermally-coupled SPTC is developed to verify the above theoretical analyses. The four-stage SPTC reaches a no-load temperature of 4.50 K and achieves cooling capacities of 10.5 W/ 80 K, 8.6 W/ 60 K, 1.5W/ 30 K and 10 mW/ 5 K.

6. References

- [1] Radebaugh R. 2000 Development of the pulse tube refrigerator as an efficient and reliable cryocooler. *Proc. of Institute of Refrigeration* (London) 1999-2000.
- [2] Dang HZ. 2015 Development of high performance moving-coil linear compressors for space Stirling-type pulse tube cryocoolers. *Cryogenics*; **68**: 1–18.
- [3] Olson J, Nast T, Evtimov B, et al., 2003 Development of a 10 K pulse tube cryocooler for space applications, *Cryocoolers* **12** 241-46.
- [4] Wilson KB and Gedeon DR, 2005 Status of pulse tube cryocooler development at Sunpower, *Cryocoolers* **13** 31-40.
- [5] Dang HZ, Bao DL, Zhang T, et al. 2018 Theoretical and experimental investigations on the three-stage Stirling-type pulse tube cryocooler using cryogenic phase-shifting approach and mixed regenerator matrices. *Cryogenics*; **93**: 7-16.
- [6] Olson J, Moore M, Champagne P, et al., 2006 Development of a space-type 4-stage pulse tube cryocooler for very low temperature, *Adv. Cryog. Eng.* **51** 623-31.
- [7] Nast T, Olson J, Roth E, et al., 2007 Development of Remote Cooling Systems for Low-Temperature, Space-Borne Systems, *Cryocoolers* **14** 33-40.

7. Acknowledgements

The work is financially supported by the Aeronautical Science Foundation of China (No. 20162490005) and the Science and Technology Commission of Shanghai Municipality (Nos. 18511110100, 18511110101, 18511110102).